

# Chromosome segregation in *Escherichia coli* division: A free energy-driven string model

J. Fan, K. Tuncay, P.J. Ortoleva\*

Center for Cell and Virus Theory, Indiana University, Bloomington, IN 47405, United States

Received 27 April 2007; accepted 6 May 2007

## Abstract

Although the mechanisms of eukaryotic chromosome segregation and cell division have been elucidated to a certain extent, those for bacteria remain largely unknown. Here we present a computational string model for simulating the dynamics of *Escherichia coli* chromosome segregation. A novel thermal-average force field accounting for stretching, bending, volume exclusion, friction and random fluctuation is introduced. A Langevin equation is used to simulate the chromosome structural changes. The mechanism of chromosome segregation is thereby postulated as a result of free energy-driven structural optimization with replication introduced chromosomal mass increase. Predictions of the model agree well with observations of fluorescence labeled chromosome loci movement in living cells. The results demonstrate the possibility of a mechanism of chromosome segregation that does not involve cytoskeletal guidance or advanced apparatus in an *E. coli* cell. The model also shows that DNA condensation of locally compacted domains is a requirement for successful chromosome segregation. Simulations also imply that the shape-determining protein MreB may play a role in the segregation via modification of the membrane pressure.

Published by Elsevier Ltd

**Keywords:** Prokaryotic cell division; Chromosome segregation; DNA compaction; *Escherichia coli*; Self-organization

## 1. Introduction

Bacteria are simple organisms which maintain precise replication, segregation and division. Although much has been understood for eukaryotic cells, how replication, segregation and division are coordinated in prokaryotic cells remains elusive. In eukaryotic cells, chromosomes are wrapped into nucleosomes around highly positively charged histone proteins, further compacted by condensing and tied by cohesions. After replication, chromosomes are separated by a dedicated cytoskeletal apparatus (Kline-Smith and Walczak, 2004). Highly conserved, histones and cytoskeletal apparatus appeared later in evolution and are not present in bacteria. Instead, bacteria appear to deploy simpler mechanisms to orchestrate precise replication, segregation and division. For example, in *Escherichia coli*, placement of the division plane is determined in combination of the MinCDE and the nucleoid occlusion systems (Norris et al., 2004; Margolin, 2006). The MinCDE system coordinates an active oscillation of Min proteins that determines the loca-

tion of *E. coli* division. Many mathematical models have been proposed to explain experimental observations (Howard et al., 2001; Meinhardt and de Boer, 2001; Kruse, 2002; Huang et al., 2003; Drew et al., 2005; Kerr et al., 2006; Pavin et al., 2006). To better understand the dynamics of chromosome replication, segregation and division, mathematical models and quantitative analysis of the mechanism is of help.

There are several hypotheses on how chromosomes segregate in bacteria. In 1963 Jacob et al. proposed a model in which bacterial chromosomes are attached to the membrane and they are separated as a result of the elongation of the membrane. As new membrane material is continuously inserted between the two attachments, the chromosomes are dragged apart (Jacob and Brenner, 1963; van Helvoort and Woldringh, 1994). Later findings on the speed of chromosome movement and cell elongation have shown that this model cannot fully explain experimental observations (Teleman et al., 1998; Daniel and Errington, 2003). In *Bacillus subtilis*, the average movement of chromosome is  $0.17 \mu\text{m min}^{-1}$ , while the speed of cell elongation is  $0.011\text{--}0.025 \mu\text{m min}^{-1}$  (Webb et al., 1998). Chromosomes move much faster than the cell elongation rate. In 2001, Lemon and Grossman proposed an extrusion capture model. A stationary replisome stays at the middle of the cell and it constantly pulls

\* Corresponding author. Tel.: +1 812 855 2717; fax: +1 812 855 8300.  
E-mail address: [ortoleva@indiana.edu](mailto:ortoleva@indiana.edu) (P.J. Ortoleva).

the mother chromosome while pushes the new daughter chromosomes away from the center (Lemon and Grossman, 2001). However, in *Caulobacter crescentus*, the replisome was found to be moving during replication (Jensen et al., 2001). In 2002, Dworkin and Losick proposed that chromosomes are repelled by RNA polymerase extending between two duplicated replication origins (*ori*) (Dworkin and Losick, 2002). However, RNA polymerase is not stationary or partially immobilized but resides everywhere around the nucleoid (Lewis et al., 2000). Woldringh presented a coupled transcription–translation–insertion (transertion) model in which daughter chromosomes compete for membrane attachment space which leads to bidirectional segregation (Woldringh, 2002). However, the model requires daughter chromosomes tethered via a different set of proteins for different space (Rocha et al., 2003) and the mechanism is too complicated to be stable enough to achieve the rapid and precise separation of DNA segments (Ronen and Sigal, 2006).

Jun and Mulder presented an entropy-driven spontaneous segregation model and they applied the model to *E. coli* and *C. crescentus* (Jun and Mulder, 2006). They considered DNA to be polymer chains and used entropy maximization to guide each bead to less crowded positions. This model successfully describes the replication-segregation process of a cell cycle. However, they introduced an inner tube (a rod shaped envelope) to restrain the mother chromosome's movement and only allowed daughter chromosomes to occupy both the inner tube and outer tube space. When replication starts, daughter chromosomes occupy the empty space outside the inner tube and are pushed toward the poles. Since the mother and daughter chromosomes consist of the same DNA material, the spatial preference should be implied by the mathematical physico-chemical model, not imposed during simulations arbitrarily. Furthermore, whether such a differential space restriction for the mother and daughter chromosomes exists awaits additional experimental evidence.

In this study we present a free energy-driven string model that neither introduces differential spatial preference nor with advanced mitotic cytoskeletal guidance. Chromosomes are organized into a string of distinct topological domains (Staczek and Higgins, 1998; Postow et al., 2004) (Fig. 1). The migration of individual domains is predicted mathematically with our model and their locations can be compared to experimental observations of loci movement. Here we present the mathematical development of the proposed free energy-driven string model and simulation results.

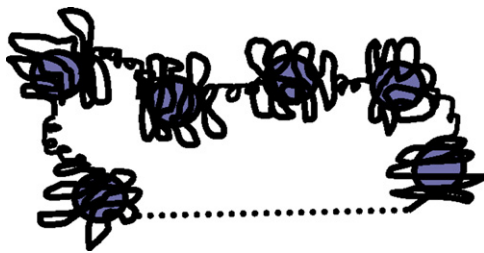


Fig. 1. Bacterial DNA organized into locally compacted–connected domains. A circular chromosome in *Escherichia coli* is thus represented as a string of interlinked domains.

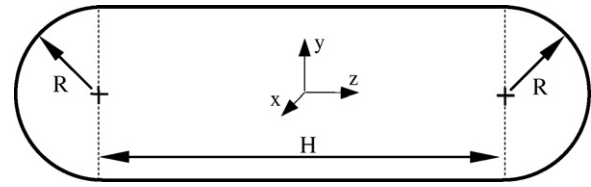


Fig. 2. The *E. coli* geometry is approximated by a cylinder of length  $H$  and two hemispheres of radius  $R$  at either end. The origin of the coordinate system ( $x$ ,  $y$ ,  $z$ ) is placed at the center of the bacterium.

## 2. Methods

### 2.1. A free energy-driven string model

To analyze the dynamics of spatial organization of chromosomes during replication and segregation, we developed a computational model to simulate the dynamics of chromosome structures over the cell cycle. The dynamics is driven by gradients of the free energy. This theme has been used to develop theories of nanoparticles, viruses and macromolecules (Miao and Ortoleva, 2006a,b).

The *E. coli* geometry is approximated by a cylinder of length  $H$  and two hemispheres of radius  $R$  at either end (Fig. 2). Chromosome movement in *E. coli* is restricted in this boundary.

We construct the free energy of the chromosomal system as follows. Two neighboring domains are assigned a stretching energy

$$U_s(d) = k_s(d - d_0)^2 \quad (\text{stretching}), \quad (1)$$

where  $k_s$  is the stretching rigidity, while  $d$  and  $d_0$  are the actual/equilibrium distances of the two linked domains. The stretching force on domain  $i$  is computed via

$$\vec{F}_i^s = -2k_s[(d_{i-1} - d_0)\vec{u}_{i-1} - (d_i - d_0)\vec{u}_i] \quad (\text{stretching}), \quad (2)$$

where  $d_i$  is the distance between domains  $i$  and  $i+1$ , and  $\vec{u}_i$  is the unit vector pointing from  $i$  to  $i+1$ .

Each domain possesses a harmonic bending potential due to its interaction with left and right neighbors

$$U_b(\theta) = k_b(\theta - \theta_0)^2 \quad (\text{bending}), \quad (3)$$

where  $k_b$  is the bending rigidity, while  $\theta$  and  $\theta_0$  are the actual/equilibrium angles between two links. The corresponding bending force on domain  $i$  is given by

$$\vec{F}_i^b = -2k_b(\vec{A}_i - \vec{B}_i + \vec{B}_{i-1} - \vec{A}_{i+1}) \quad (\text{bending}) \quad (4)$$

with

$$\vec{A}_i = (\theta_i - \theta_0) \frac{\vec{u}_i + \vec{u}_{i-1} \cos \theta_i}{d_{i-1} \sin \theta_i},$$

$$\vec{B}_i = (\theta_i - \theta_0) \frac{\vec{u}_{i-1} + \vec{u}_i \cos \theta_i}{d_i \sin \theta_i}. \quad (5)$$

Since distances between domains are much larger than the van der Waals interaction range or the electrostatic Debye length of the intracellular medium, we approximate these interactions by a

short-range excluded volume interaction potential as proposed to predict chromosome structures (Munkel and Langowski, 1998):

$$U_e(r) = k_e \left( 1 + \frac{r^4 - 2r_c^2 r^2}{r_c^4} \right) \quad (\text{excluded volume}), \quad (6)$$

where  $k_e$  is the excluded volume coefficient, while  $r$  and  $r_c$  are the actual and cut-off distances between two domains. All domains with a distance  $r$  to domain  $i$  contribute a force on domain  $i$ :

$$\vec{F}_i^e = \sum_{j \neq i} 4k_e \frac{(r_{ji}^2 - r_c^2) \vec{r}_{ji}}{r_c^4} \quad (\text{excluded volume}), \quad (7)$$

where  $r_{ji}$  is the distance between  $j$  and  $i$  ( $r_{ji} \leq r_c$ ).

To keep bacterial DNA inside the cell and simulate the effect of membrane pressure, a boundary force is introduced:

$$\vec{F}_i^m = k_m \frac{\vec{n}_{mi}}{r_{mi}^2} \quad (\text{membrane pressure}), \quad (8)$$

where  $k_m$  is the membrane pressure coefficient,  $r_{mi}$  the nearest distance from the membrane to domain  $i$ , and  $\vec{n}_{mi}$  is the unit vector pointing from the nearest membrane point to domain  $i$ .

To account for energy exchange between a given domain and the solution or the other domains, a friction force is introduced:

$$\vec{F}_i^f = -k_f \vec{v}_i \quad (\text{friction force}), \quad (9)$$

where  $k_f$  is the friction coefficient and  $\vec{v}_i$  is the velocity of domain  $i$ .

A small random force is introduced to account for fluctuations in the system and to avoid being locked in states of local energy minima. The random force ( $\vec{F}_i^r$ ) is generated in all directions at every time step via

$$\vec{F}_i^r = k_r \vec{\varepsilon} \quad (\text{fluctuation force}), \quad (10)$$

where  $\vec{\varepsilon}$  is a vector, each of whose three components is chosen independently and at random subject to the interval  $(-1,1)$ .

Assuming inertial forces are small compared to frictional forces, the position and velocity of each domain is calculated over time  $t$  via numerical simulation of Langevin equations:

$$\frac{d\vec{r}}{dt} = \vec{v}_i, \quad (11)$$

$$k_f \vec{v}_i = \vec{F}_i, \quad (12)$$

where  $\vec{F}_i$  is the sum of all forces (except friction) on  $i$ .

With the above Langevin dynamics, along with the elongation of cell (i.e.  $H$  increases over time) and events of replication, we simulated the cycle of *E. coli* elongation and chromosome replication and segregation. For domains undergoing replication, they are unwound by replisomes before replication and then refolded after replication is over. Thus bending force of replicating domains is missing temporally and the stretching force is weakened in the unwinding state. After replication of each domain, daughter domains are assigned to the same position as of their mother domain. In subsequent time steps, they are positioned appropriately by the force field.

## 2.2. Simulation parameters and model details

To test the free energy-driven string model, parameter values were chosen based on available experimental data. In a culture medium of fixed nutrition level, *E. coli* elongates with fixed width (Marr et al., 1966). In our numerical simulations, we used  $R = 0.5 \mu\text{m}$  as the cell radius and elongated  $H$  from  $2.0 \mu\text{m}$  to  $4.0 \mu\text{m}$  in one cell cycle. The elongation rate of cell membrane was kept constant at  $0.025 \mu\text{m min}^{-1}$ . A slow growth condition was used to simplify the model (i.e. only one initiation of replication occurs per cell cycle). The cell doubling time was taken to be 80 min: 20 min before initiation of chromosome replication, 40 min between initiation and completion of chromosome replication, and 20 min for post preparation of segregation and division.

The *E. coli* chromosome consists of 4.6 million base pairs and is compacted into a circular ring of topological domains. Recent studies of florescent tracking of loci movement show that loci  $\sim 200$  kbp apart can occupy separate positions in the cell and segregate independently (Viollier et al., 2004; Fekete and Chatteraj, 2005). Thus we used 22 locally compacted domains in our simulations to represent a complete chromosome. The average size of a domain is 210 kbp.

The stretching rigidity of DNA has been actively studied over the past decade (Bustamante et al., 2003). The physical properties of a DNA strand can be approximated using a worm-like chain (WLC) model. However, the detailed configuration of DNA that links two domains is still unresolved. We assume the stretching rigidity could be approximated as  $k_B T/A$ , where  $k_B$  is Boltzmann's constant,  $T$  is absolute temperature and  $A$  is the flexural persistence length (Bustamante et al., 2003). We used a stretching rigidity of  $k_s = 60 k_B T \mu\text{m}^{-2}$  (Munkel and Langowski, 1998) and an equilibrium link distance of  $d_0 = 0.1 \mu\text{m}$  in our simulation as a rough estimate (van den Engh et al., 1992). In the unwinding state, the stretching rigidity is weakened to  $0.06 k_B T \mu\text{m}^{-2}$ . We used an angle of  $70^\circ$  as the equilibrium harmonic bending angle since protein FIS in *E. coli* bends DNA with an angle between  $50^\circ$  and  $90^\circ$  upon binding (Altuvia et al., 1994; Stavans and Oppenheim, 2006). The bending rigidity was approximated as  $k_b = 0.75 k_B T$ . The cut-off distance of the volume exclusive effect was taken to be  $r_c = 0.4 \mu\text{m}$  and the volume exclusive coefficient is  $k_e = 1.5 k_B T$ . We used a membrane pressure force coefficient of  $k_m = 0.05 k_B T \mu\text{m}$  and a friction coefficient of  $k_f = 35 k_B T \mu\text{m}^{-2} \text{s}$ . The amplitude of the random force was taken to be  $k_r = 0.001 k_B T \mu\text{m}^{-1}$ .

With the above six force fields (stretching, bending, volume exclusion, membrane pressure, friction and fluctuation), we simulated *E. coli* self-organized chromosomal structural segregation over one cell cycle. The forces are all essential as any subset of them alone cannot reproduce the segregation correctly. Without the stretching force, chromosome domains are disconnected and become scattered across the cell. Without the bending force, structural details of angles between nearby domains are missed and the segregated chromosomes cannot maintain correct loci configurations (i.e. a mother chromosome with the *ori* region in its center may produce daughters with the *ori* regions close to the poles). Without the volume exclusion force, chromosomes

become so entangled that they cannot segregate. Membrane pressure keeps chromosomes inside the cell and helps segregate daughter chromosomes further apart and tends to retain structural loci configuration. Without the friction force, domains oscillate in large amplitude around their equilibrium positions and the system is highly unstable. Without the random force, the system may be locked up in unstable states or local minima.

### 3. Results and discussion

The simulation was started at the equilibrium configurations and such that the *ori* and *ter* domains are close to the cell center, while the left and right arms of the chromosome resided in the two cell halves (Nielsen et al., 2006a,b). Simulated chromosomal structures at various stages of the cell cycle are shown in Fig. 3. During the first 20 min there was only one chromosome. At the 20th min the *ori* domain was unwound and replication was initiated. Once the *ori* domain was replicated, two daughter *ori* domains were formed by DNA recompaction near the position of the mother domain was located. Over the next 40 min, domains in the mother chromosome were replicated sequentially and bidirectionally until all domains were replicated. In the last 20 min, the daughter chromosomes were physically unconnected and separated. Before the final septum formed at the cell equator, the two chromosomes created a low concentration area of nucleoid in the mid-cell which is noted as one of the independent forces to position the cell division plane (Sun and Margolin, 2001).

To track the positions of the *ori* domains during replication-segregation, we colored the *ori* domains in green in Fig. 3. Before initiation of replication, there was only one *ori* domain close to the middle of the cell. Then the mother *ori* domain was replicated into two daughter *ori* domains. As replication continued, the two daughter *ori* domains moved apart toward opposite poles. After completion of replication, the two *ori* domains relocated to the middle of the two daughter chromosomes. The *ter* domain was replicated after the *ori* domains had been fully apart. The locations of the *ori* and *ter* domains during the cell cycle are shown in Fig. 4. The daughter chromosomes migrated to the left and right cell halves as they reorganized into their final configurations. At the end of replication-segregation, topology of chromosomal structures was faithfully inherited from the mother cell into the new generation.

Hansen and colleagues used a fine-tuned GFP-*parB/parS* system to label the loci and recorded their positions over a cell cycle (Nielsen et al., 2006a). Our simulation reproduced many of their observations. For example, they reported that the *ori* region segregation displays a noticeable delay after replication. We predict a similar phenomenon wherein the *ori* domains tend to be colocalized longer than the other domains after they are replicated (Fig. 4). This is due to the closeness of the left and right neighbors of the *ori* domain when the *ori* domain was being replicated. Since both of the replicated *ori* regions are connected to the same neighbor domains transiently, they are tied to a position close to each other for a small period. However, when the *ter* domain was replicated, the left and right domains were on different daughters. Hence the two newly replicated *ter* domains moved quickly

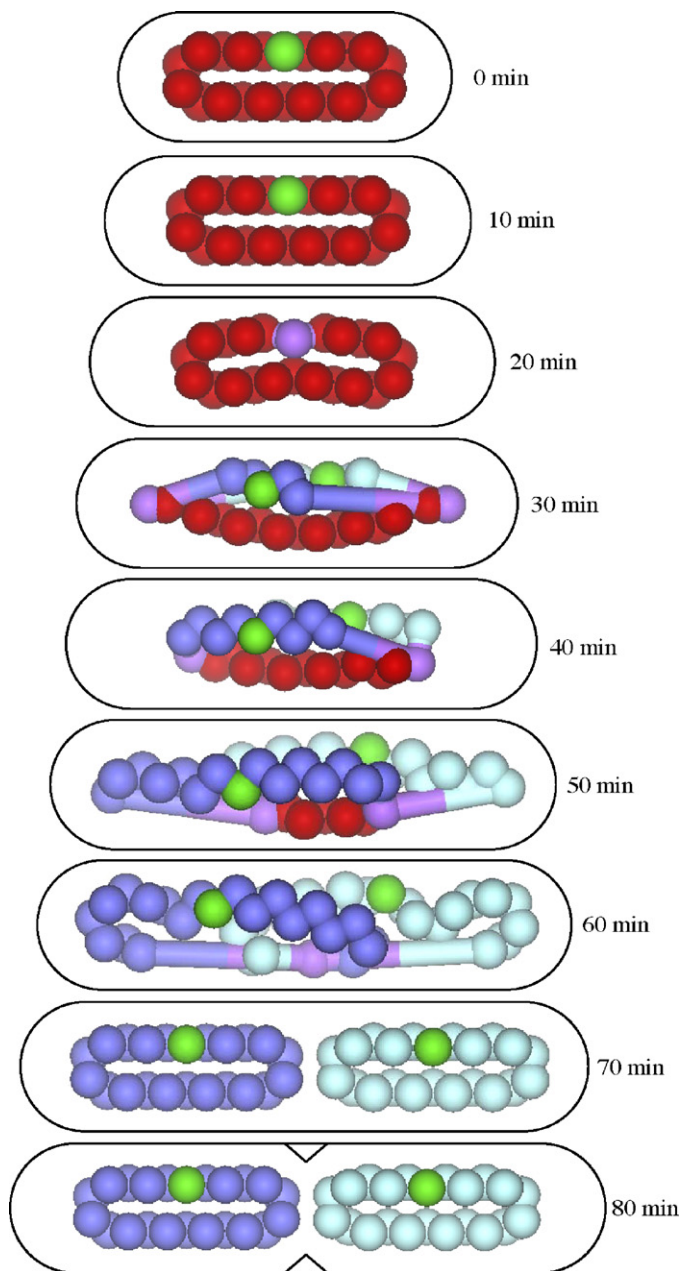


Fig. 3. Simulated configuration of *E. coli* chromosome structures. Green beads are domains that contain the *ori* region. Purple beads are domains undergoing replication. Red beads are domains of mother chromosome. Cyan and blue beads are domains of the two daughter chromosomes.

apart to their respective daughter chromosomes. The separation speed of *ter* domains was faster than that of *ori* domains. Positions of selected domains containing the loci studied by Hansen and colleagues are plotted in Fig. 5. The overall behavior of our simulated loci migration is similar to their observations. The *ori* domains separate near the cell center and they move slowly outward until they reach the cell quarter positions. Intermediate loci are segregated from positions that are away from the center. However, the segregation of some early replicated domains seems faster in Hansen's chart than those in our simulated results. We believe that it is because foci close to each other may not be identifiable as distinct spots in experimental measurements.

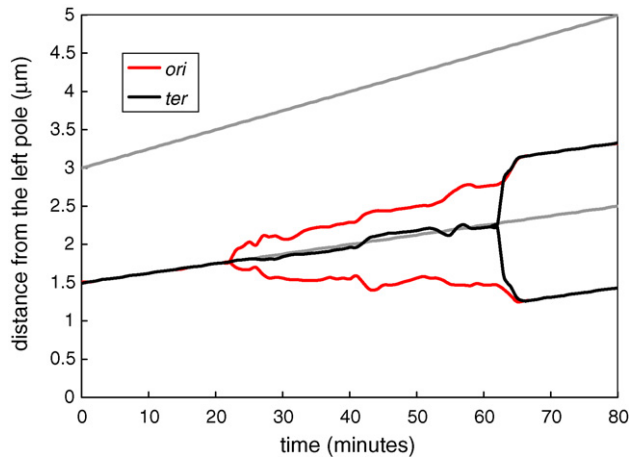


Fig. 4. Location of the *ori* and *ter* regions over an *E. coli* cell cycle. The two regions are located near the middle of the cell before initiation of replication. After replication, the two regions move toward the two opposite poles and finally localize near the quarter-cell positions.

Only foci that are apart far enough were reported as separated spots in Hansen's chart. Also since cells may not initiate replication exactly at the same cell length, the mapping from cell length to cell cycle time in the experimental chart introduced errors (Nielsen et al., 2006a). During the structural reorganization process, locations of domains fluctuated in the space and may have fast movement. The speed of loci movement usually maximizes right after their replication. The maximum speed of domain movement in our simulation is about  $0.6 \mu\text{m min}^{-1}$ . As maximum chromosome foci movement has been observed to be  $0.5 \mu\text{m}$  in a matter of seconds (Nielsen et al., 2006a) and many loci can move  $1 \mu\text{m}$  apart in 2 min right after their replication (Viollier et al., 2004), our speed of loci movement is reasonable.

Sherratt and coworkers monitored the position of the *ter* region in a population of cells that had duplicated the *ter* region and were approaching cell division (Wang et al., 2005). They reported that 97% of sister nucleoids pairs exhibited asymmet-

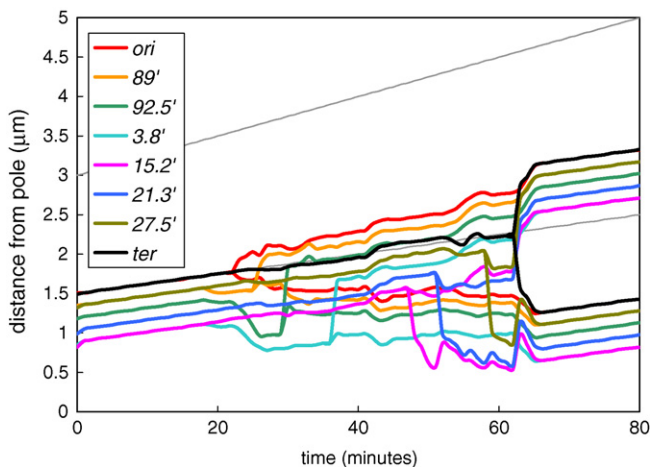


Fig. 5. Predicted migration of loci in a cell cycle. The loci picked are from the work of Hansen and colleagues (Nielsen et al., 2006a). Loci positions are calculated from the distance to the nearest pole as Hansen et al. prepared their experimental chart.

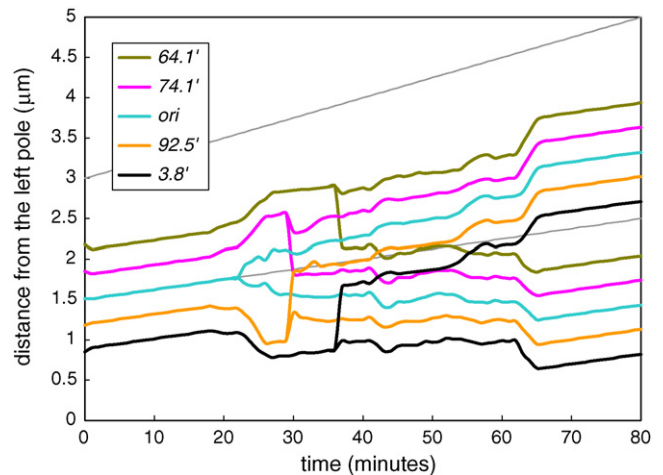


Fig. 6. Migration of loci in the left and right chromosome arms and the center. The single *E. coli* chromosome is organized with the left and right chromosome arms in separate cell halves. After replication and segregation, the relative position of individual chromosome loci is preserved. The cell exhibits a “left-right-left-right” pattern before cell division which is in agreement with observations.

ric segregation in *E. coli*. Furthermore, in filamental cells that contain four or eight nucleoids, the majority of them had the asymmetric pattern polarized throughout the filament. In a cell just prior to division, the arrangement of left and right arms of chromosome is “left-right-septum-left-right” and in a filamental cell is “left-right-left-right-left-right-left-right...”. We ran a simulation with initial configuration of the left and right chromosome arms in the left and right cell halves as observed in the experiments (Nielsen et al., 2006b). The simulated migration paths of 5 individual loci along the chromosome, 2 left arm loci (64.1' and 74.1'), 2 right arm loci (92.5' and 3.8') and the mid-cell *ori* loci (84.3'), are shown in Fig. 6. At the end of the replication-segregation, the spatial configuration of chromosomal loci is the same as the mother chromosome. The *E. coli* cell before division exhibited a “left-right-left-right” polarized asymmetric pattern which is in agreement with experimental observations.

Earlier studies of chromosomal loci positions proposed that the *ori* and *ter* regions are located near the two opposite poles of *E. coli* in newly divided cells. Before the initiation of replication, the *ori* and *ter* regions move to mid-cell. After replication, the *ori* and *ter* regions move back to the poles (Niki and Hiraga, 1998; Niki et al., 2000; Bates and Kleckner, 2005). However, in recent studies it is proposed that the *ori* and *ter* regions remain near the center of the cell before replication and move to quarter positions after replication (Wang et al., 2005; Nielsen et al., 2006a,b). We adopted the most recent findings so that the *ori* and *ter* domains were located near cell center while the left and right arms were placed in the two cell halves before the initiation of replication. We also tested the initial configuration with the *ori* and *ter* domains close to cell poles. The simulated results with polar positioned *ori* and *ter* domains showed that the chromosomes can segregate but the loci migration path does not agree with experimental *E. coli* observations (Nielsen et al., 2006a). After the *ori* domain has been replicated at the pole,

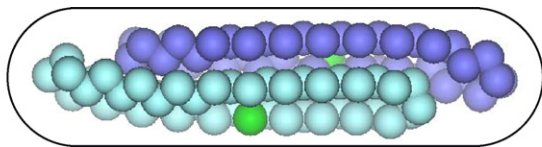


Fig. 7. Simulated *E. coli* chromosome structure with double number of domains representing a chromosome (each domain size is half of the normal). The chromosomes are entangled and therefore cannot segregate readily. Shown is the configuration just before division. Here green beads are domains containing *ori* region. The two daughter chromosomes are colored in cyan and blue.

one newly replicated *ori* domain moved toward cell center and stayed there after replication has finished. The other *ori* domain remained at the original pole during the whole process. When the *ter* domain was replicated at its original pole, one newly replicated *ter* domain moved quickly to the cell center while the other remained at the pole. The orientation of chromosomal structures was thus preserved after replication. In *C. crescentus*, the *ori* and *ter* domains are at two poles before replication initiation. But after the *ori* domain is replicated, one newly replicated *ori* domain moves rapidly to the opposite pole and stays there (Jensen et al., 2001; Viollier et al., 2004; Thanbichler et al., 2005). Just before cell division, the chromosomes exhibit a “*ori-ter-septum-ter-ori*” configuration. It is proposed that some polar localizing proteins may function in *C. crescentus* to tether the *ori* regions to both poles (Mohl and Gober, 1997; Jacobs et al., 1999).

Sufficient compaction of chromosome plays an important role in chromosome segregation. The *E. coli* DNA is compacted by supercoiling (DNA gyrase), small nucleoid-associated proteins (H-NS, HU, etc.) and SMC-like complexes (MukBEF). The HU and H-NS are histone-like proteins that assemble DNA into nucleoprotein complexes. Certain mutations in the genes encoding HU and H-NS cause nucleoids partition defects (Huisman et al., 1989; Dri et al., 1991; Kaidow et al., 1995). Mutations in *mukB* of *E. coli* result in chromosome decompaction and irregular distribution of nucleoids along an elongated cell (Niki et al., 1991, 1992). To test whether chromosome compaction is a requirement for segregation, we constructed a model with twice as many domains representing a chromosome (the size of each distinct domain is half of the normal). As shown in Fig. 7, our result shows the two daughter chromosomes remain entangled together after replication. There is no nucleoid-empty area at mid-cell. Hence, the *E. coli* chromosomes cannot form a preferred cell division plane at mid-cell. This will generate a nucleoid cells or elongated (filamental) cells without division. The prediction is consistent with observations on cells with mutant compaction genes (Huisman et al., 1989; Dri et al., 1991; Niki et al., 1991, 1992; Kaidow et al., 1995). However, by compacting DNA into fewer domains (increase domain size while keeping all the other parameters same), our model shows that chromosomes can segregate successfully. It can leave excessive nucleoid empty areas around the mid-cell and in the two poles. Furthermore, the two daughter chromosomes may not precisely be located at the quarter-cell positions after segregation (one is close to the middle while the other is in the quarter).

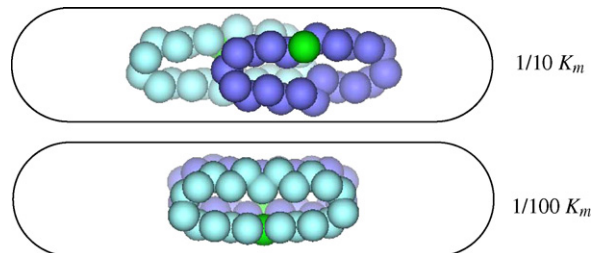


Fig. 8. Simulated results of *E. coli* chromosome structure with decreased membrane pressure coefficient (10-fold smaller and 100-fold smaller). Chromosomes become wider in the radial direction of the cell and both cells cannot segregate in agreement with observations. Here green beads are domains that contains *ori* region. The rest of the domains of two daughter chromosomes are colored in cyan and blue, respectively.

Recent studies show that cell shape-determining protein MreB plays an important role in chromosome segregation (Kruse et al., 2003, 2005; Figge et al., 2004). The *E. coli* cell membrane imposes high pressure on chromosomes inside the cell (Odijk, 2000). If the membrane is lysed, DNA can “explode” out of the cell (Odijk, 2000) with a liberated volume of 100-fold (Cunha et al., 2005). The MreB protein of *E. coli* forms helical filaments beneath the cell surface and maintains the cell in a rod-shape (Kruse et al., 2003). Depletion of MreB results in spherical or enlarged cells and unsuccessful segregations (Kruse et al., 2003). Thus we hypothesize that a decrease in cell membrane pressure might cause the segregation defects in MreB depleted cells. We simulated a 10-fold smaller membrane pressure coefficient case with the same cell size in our model. The simulated chromosome structures before cell division are shown in Fig. 8. As membrane pressure decreases, the chromosomes become wider in the radial direction of the cell. The spatial configuration of each chromosome tends to be circular and the chromosomes movement space is enlarged. These results indicate a random localization of *ori* regions is more likely in the MreB depleted daughter cells than in the wild-type cells. The simulated results also indicate the two daughter chromosomes cannot segregate as observed experimentally. When the membrane pressure coefficient was further decreased to 100-fold, the two daughter chromosomes stayed side by side in parallel (Fig. 8). The pair up of daughter chromosomes is observed in rich medium of MreB depleted cells (Kruse et al., 2003). We also simulated a situation of 10-fold larger membrane pressure coefficient in our model. The simulation results showed that domains became clustered toward the cell center but segregation was successfully accomplished; in agreement with observations that over expression of wild-type MreB does not perturb chromosome segregation (Kruse et al., 2003). However, with a 100-fold larger membrane pressure coefficient, chromosomes failed to segregate as the pressure is too large.

#### 4. Conclusion

A free energy-driven chromosome structural optimization approach that simulates the *E. coli* replication-segregation cell cycle is presented. The model uses a string of topologically compacted domains to represent the chromosome structure. The

movement of individual domains is guided by a force field accounting for stretching, bending, volume exclusion, membrane pressure, friction, and random fluctuations. The elongation of cell membrane and sequential replication of domains are accounted for in the model. Migration of individual loci simulated in our model agrees well with experimental observations. The simulated results indicate *E. coli* chromosomes may segregate without external help if chromosomes are well compacted into topological domains. It is also noticed that membrane pressure plays an important role in maintaining faithful heritage of loci positions as of perturbation of the shape-determining protein MreB.

## Acknowledgements

We thank the U.S. Department of Energy and the Indiana University College of Arts and Sciences for their support of the Center for Cell and Virus Theory that helped facilitate this research.

## References

- Altuvia, S., Almiron, M., Huisman, G., Kolter, R., Storz, G., 1994. The dps promoter is activated by OxyR during growth and by IHF and sigma S in stationary phase. *Mol. Microbiol.* 13, 265–272.
- Bates, D., Kleckner, N., 2005. Chromosome and replisome dynamics in *E. coli*: loss of sister cohesion triggers global chromosome movement and mediates chromosome segregation. *Cell* 121, 899–911.
- Bustamante, C., Bryant, Z., Smith, S.B., 2003. Ten years of tension: single-molecule DNA mechanics. *Nature* 421, 423–427.
- Cunha, S., Woldringh, C.L., Odijk, T., 2005. Restricted diffusion of DNA segments within the isolated *Escherichia coli* nucleoid. *J. Struct. Biol.* 150, 226–232.
- Daniel, R.A., Errington, J., 2003. Control of cell morphogenesis in bacteria: two distinct ways to make a rod-shaped cell. *Cell* 113, 767–776.
- Drew, D.A., Osborn, M.J., Rothfield, L.I., 2005. A polymerization–depolymerization model that accurately generates the self-sustained oscillatory system involved in bacterial division site placement. *Proc. Natl. Acad. Sci. U.S.A.* 102, 6114–6118.
- Dri, A.M., Rouviere-Yaniv, J., Moreau, P.L., 1991. Inhibition of cell division in hupA hupB mutant bacteria lacking HU protein. *J. Bacteriol.* 173, 2852–2863.
- Dworkin, J., Losick, R., 2002. Does RNA polymerase help drive chromosome segregation in bacteria? *Proc. Natl. Acad. Sci. U.S.A.* 99, 14089–14094.
- Fekete, R.A., Chattoraj, D.K., 2005. A cis-acting sequence involved in chromosome segregation in *Escherichia coli*. *Mol. Microbiol.* 55, 175–183.
- Figge, R.M., Divakaruni, A.V., Gober, J.W., 2004. MreB, the cell shape-determining bacterial actin homologue, co-ordinates cell wall morphogenesis in *Caulobacter crescentus*. *Mol. Microbiol.* 51, 1321–1332.
- Howard, M., Rutenberg, A.D., de Vet, S., 2001. Dynamic compartmentalization of bacteria: accurate division in *E. coli*. *Phys. Rev. Lett.* 87, 278102.
- Huang, K.C., Meir, Y., Wingreen, N.S., 2003. Dynamic structures in *Escherichia coli*: spontaneous formation of MinE rings and MinD polar zones. *Proc. Natl. Acad. Sci. U.S.A.* 100, 12724–12728.
- Huisman, O., Faelen, M., Girard, D., Jaffe, A., Toussaint, A., Rouviere-Yaniv, J., 1989. Multiple defects in *Escherichia coli* mutants lacking HU protein. *J. Bacteriol.* 171, 3704–3712.
- Jacob, F., Brenner, S., 1963. On the regulation of DNA synthesis in bacteria: the hypothesis of the replicon. *C. R. Hebd. Seances. Acad. Sci.* 256, 298–300.
- Jacobs, C., Domian, I.J., Maddock, J.R., Shapiro, L., 1999. Cell cycle-dependent polar localization of an essential bacterial histidine kinase that controls DNA replication and cell division. *Cell* 97, 111–120.
- Jensen, R.B., Wang, S.C., Shapiro, L., 2001. A moving DNA replication factory in *Caulobacter crescentus*. *EMBO J.* 20, 4952–4963.
- Jun, S., Mulder, B., 2006. Entropy-driven spatial organization of highly confined polymers: lessons for the bacterial chromosome. *Proc. Natl. Acad. Sci. U.S.A.* 103, 12388–12393.
- Kaidow, A., Wachi, M., Nakamura, J., Magae, J., Nagai, K., 1995. Anucleate cell production by *Escherichia coli* delta hns mutant lacking a histone-like protein H-NS. *J. Bacteriol.* 177, 3589–3592.
- Kerr, R.A., Levine, H., Sejnowski, T.J., Rappel, W.J., 2006. Division accuracy in a stochastic model of min oscillations in *Escherichia coli*. *Proc. Natl. Acad. Sci. U.S.A.* 103, 347–352.
- Kline-Smith, S.L., Walczak, C.E., 2004. Mitotic spindle assembly and chromosome segregation: refocusing on microtubule dynamics. *Mol. Cell* 15, 317–327.
- Kruse, K., 2002. A dynamic model for determining the middle of *Escherichia coli*. *Biophys. J.* 82, 618–627.
- Kruse, T., Moller-Jensen, J., Lobner-Olesen, A., Gerdes, K., 2003. Dysfunctional MreB inhibits chromosome segregation in *Escherichia coli*. *EMBO J.* 22, 5283–5292.
- Kruse, T., Bork-Jensen, J., Gerdes, K., 2005. The morphogenetic MreBCD proteins of *Escherichia coli* form an essential membrane-bound complex. *Mol. Microbiol.* 55, 78–89.
- Lemon, K.P., Grossman, A.D., 2001. The extrusion-capture model for chromosome partitioning in bacteria. *Genes Dev.* 15, 2031–2041.
- Lewis, P.J., Thaker, S.D., Errington, J., 2000. Compartmentalization of transcription and translation in *Bacillus subtilis*. *EMBO J.* 19, 710–718.
- Margolin, W., 2006. Bacterial division: another way to box in the ring. *Curr. Biol.* 16, R881–R884.
- Marr, A.G., Harvey, R.J., Trentini, W.C., 1966. Growth and division of *Escherichia coli*. *J. Bacteriol.* 91, 2388–2389.
- Meinhardt, H., de Boer, P.A., 2001. Pattern formation in *Escherichia coli*: a model for the pole-to-pole oscillations of Min proteins and the localization of the division site. *Proc. Natl. Acad. Sci. U.S.A.* 98, 14202–14207.
- Miao, Y., Ortoleva, P., 2006a. All-atom multiscale and new ensembles for dynamical nanoparticles. *J. Chem. Phys.* 125, 44901.
- Miao, Y., Ortoleva, P.J., 2006b. Viral structural transitions: an all-atom multiscale theory. *J. Chem. Phys.* 125, 214901.
- Mohl, D.A., Gober, J.W., 1997. Cell cycle-dependent polar localization of chromosome partitioning proteins in *Caulobacter crescentus*. *Cell* 88, 675–684.
- Munkel, C., Langowski, J., 1998. Chromosome structure predicted by a polymer model. *Phys. Rev. E* 57, 5888–5896.
- Nielsen, H.J., Li, Y., Youngren, B., Hansen, F.G., Austin, S., 2006a. Progressive segregation of the *Escherichia coli* chromosome. *Mol. Microbiol.* 61, 383–393.
- Nielsen, H.J., Ottesen, J.R., Youngren, B., Austin, S.J., Hansen, F.G., 2006b. The *Escherichia coli* chromosome is organized with the left and right chromosome arms in separate cell halves. *Mol. Microbiol.* 62, 331–338.
- Niki, H., Hiraga, S., 1998. Polar localization of the replication origin and terminus in *Escherichia coli* nucleoids during chromosome partitioning. *Genes Dev.* 12, 1036–1045.
- Niki, H., Jaffe, A., Imamura, R., Ogura, T., Hiraga, S., 1991. The new gene mukB codes for a 177 kd protein with coiled-coil domains involved in chromosome partitioning of *E. coli*. *EMBO J.* 10, 183–193.
- Niki, H., Imamura, R., Kitaoka, M., Yamanaka, K., Ogura, T., Hiraga, S., 1992. *E. coli* MukB protein involved in chromosome partition forms a homodimer with a rod-and-hinge structure having DNA binding and ATP/GTP binding activities. *EMBO J.* 11, 5101–5109.
- Niki, H., Yamaichi, Y., Hiraga, S., 2000. Dynamic organization of chromosomal DNA in *Escherichia coli*. *Genes Dev.* 14, 212–223.
- Norris, V., Woldringh, C., Mileykovskaya, E., 2004. A hypothesis to explain division site selection in *Escherichia coli* by combining nucleoid occlusion and Min. *FEBS Lett.* 561, 3–10.
- Odijk, T., 2000. Dynamics of the expanding DNA nucleoid released from a bacterial cell. *Physica A* 277, 62–70.
- Pavin, N., Paljetak, H.C., Krstic, V., 2006. Min-protein oscillations in *Escherichia coli* with spontaneous formation of two-stranded filaments in a three-dimensional stochastic reaction–diffusion model. *Phys. Rev. E: Stat. Nonlin. Soft. Matter Phys.* 73, 021904.
- Postow, L., Hardy, C.D., Arsuaga, J., Cozzarelli, N.R., 2004. Topological domain structure of the *Escherichia coli* chromosome. *Genes Dev.* 18, 1766–1779.

- Rocha, E.P., Fralick, J., Vedyappan, G., Danchin, A., Norris, V., 2003. A strand-specific model for chromosome segregation in bacteria. *Mol. Microbiol.* 49, 895–903.
- Ronen, H., Sigal, B.Y., 2006. Resolving chromosome segregation in bacteria. *J. Mol. Microbiol. Biotechnol.* 11, 126–139.
- Staczek, P., Higgins, N.P., 1998. Gyrase and Topo IV modulate chromosome domain size in vivo. *Mol. Microbiol.* 29, 1435–1448.
- Stavans, J., Oppenheim, A., 2006. DNA–protein interactions and bacterial chromosome architecture. *Phys. Biol.* 3, R1–R10.
- Sun, Q., Margolin, W., 2001. Influence of the nucleoid on placement of FtsZ and MinE rings in *Escherichia coli*. *J. Bacteriol.* 183, 1413–1422.
- Teleman, A.A., Graumann, P.L., Lin, D.C., Grossman, A.D., Losick, R., 1998. Chromosome arrangement within a bacterium. *Curr. Biol.* 8, 1102–1109.
- Thanbichler, M., Viollier, P.H., Shapiro, L., 2005. The structure and function of the bacterial chromosome. *Curr. Opin. Genet. Dev.* 15, 153–162.
- van den Engh, G., Sachs, R., Trask, B.J., 1992. Estimating genomic distance from DNA sequence location in cell nuclei by a random walk model. *Science* 257, 1410–1412.
- van Helvoort, J.M., Woldringh, C.L., 1994. Nucleoid partitioning in *Escherichia coli* during steady-state growth and upon recovery from chloramphenicol treatment. *Mol. Microbiol.* 13, 577–583.
- Viollier, P.H., Thanbichler, M., McGrath, P.T., West, L., Meewan, M., McAdams, H.H., Shapiro, L., 2004. Rapid and sequential movement of individual chromosomal loci to specific subcellular locations during bacterial DNA replication. *Proc. Natl. Acad. Sci. U.S.A.* 101, 9257–9262.
- Wang, X., Possoz, C., Sherratt, D.J., 2005. Dancing around the divisome: asymmetric chromosome segregation in *Escherichia coli*. *Genes Dev.* 19, 2367–2377.
- Webb, C.D., Graumann, P.L., Kahana, J.A., Teleman, A.A., Silver, P.A., Losick, R., 1998. Use of time-lapse microscopy to visualize rapid movement of the replication origin region of the chromosome during the cell cycle in *Bacillus subtilis*. *Mol. Microbiol.* 28, 883–892.
- Woldringh, C.L., 2002. The role of co-transcriptional translation and protein translocation (transertion) in bacterial chromosome segregation. *Mol. Microbiol.* 45, 17–29.